Asian Journal of Civil Engineering
https://doi.org/10.1007/s42107-022-00467-3

RESEARCH

Experimental investigation of ferrocement sandwich composite jack arch slab

Ahmed Hatif Obaid[1] · **Abdulkhaliq A. Jaafer**[1]

Received: 10 April 2022 / Accepted: 1 June 2022

Abstract
The aim of this study is to propose a new, sustainable, and effective method for the construction of jack-arch slabs. The main idea of this method is to produce lightweight precast ferrocement elements in the form of sandwich panels to be used in the jack-arch slab between the steel I-section beam. In this study, eight specimens were manufactured and tested under three-point loads. The specimens are made of two ferrocement layers of 15 mm in thickness, separated by core material prisms (200 × 100 × 100) mm. Two different core materials are used; these are styropor or cellular concrete block (thermostone). The precast ferrocement sandwich slab has a section depth of 130 mm (15 mm for each ferrocement layer and 100 mm for the prisms). One of the specimens is made of clay brick and gypsum mortar to represent a traditional jack-arch slab and is employed as a control. The remaining seven specimens are ferrocement sandwich composite slabs. The ferrocement laminates consist of four layers of steel wire mesh embedded in a high-flowable cement mortar of 68 MPa compressive strength. The main variables considered in the study were the type of core material (styropor or cellular concrete), span length, section depth of the slab, and shear connectors. The results regarding the ultimate loads and ductility showed that all precast ferrocement sandwich slab specimens had a higher than the control by (471.23–1216.89%) and (60.55–205.50%), respectively. Using steel wire of 3 mm diameter as shear connectors improved the ultimate loads and ductility by (863.01–1216.89%) and (96.33–205.50%), respectively, over the control specimen. The ultimate load and ductility index are improved by 77.48 and 14.28% when section depth is increased from 130 to 160 mm, respectively. Ferrocement sandwich composite slab specimens have higher flexural strength and modulus than the control specimen by a range of (579.16–1231.25%) and (65.05–247.91%), respectively. The reduction in weight of the sandwich slabs compared to the traditional jack arch reached 43.13% for the styropor core material. The modes of failure showed that the ferrocement sandwich slabs have a ductile behavior. According to the encouraging results of the study, the proposed ferrocement sandwich slab can be used as an alternative to the traditional brick-work slab.

Keywords Jack arch slab · Ferrocement · Shear connector · Sandwich

Introduction

Jack arch slabs are brick slabs supported by steel (I-section) beams that rest on load-bearing walls or lintels with 70–90 cm centers. The spans between steel I-section beams are built with clay brick units that are bonded together by gypsum mortar as a binder due to its quick setting. For the first time, Victorian architects in Britain developed the jack arch slab. After that, the jack-arch slab spread to most countries, including North America, East Europe, and India. By the mid-twentieth century, it had become a popular flooring system in several Middle Eastern countries, such as Iran and Iraq. Arching with bricks was a well-known technique that was usually employed in Iraq. Despite the widespread use of reinforced concrete in construction slabs, arch brick slabs are still used in many countries, especially in Iraqi regions, due to their speed of construction, low cost, no need for skilled labor, no need for complex engineering calculations, effectiveness for small areas, and absence of mold, reinforcement, casting and curing. People with low finances usually employ the arch brick slab. Cellular concrete block units were often noticed to be used in the

✉ Ahmed Hatif Obaid
aobaid@uomisan.edu.iq

Abdulkhaliq A. Jaafer
aljabery@uomisan.edu.iq

1 Department of Civil Engineering, University of Misan, Maysan, Iraq

construction of jack arch slabs due to speed of work, thermal insulation, and lightweight see Fig. 1. Despite the general advantages of a jack-arch slab, there are some drawbacks. In particular, as a primitive building technique, it sustains limited loads, is sensitive to seismic loadings, and uses gypsum mortar as a binder, which has low moisture resistance. The jack arch slab structure is safe under normal static loading because the brick arches carry gravity loads mostly in compression along the arch towards the beams. Through parallel steel beams, the load is then transmitted to walls or beams. The jack-arch slab method was normally regarded as a one-way slab because of its geometric shape (Maheri et al., 2012). Possible problems with ordinary one-way jack-arch slabs were investigated. Maheri and Rahmani proposed a novel two-way technique in 2003. The proposed technique uses a sequence of transverse steel beams between the main I-beams. This system allows transmission of the vertical load in two directions. The proposed technique found that diaphragm action and resistance to gravity and seismic loads were improved (Maheri & Rahmani, 2003). Experimentally investigated the effect of using a concrete overlay layer on top of the jack arch slab. The results revealed that the jack arch slab's strength and ductility, as well as its seismic performance, were enhanced (Pourfallah et al., 2009). Resan and Dawood studied the performance of jack-arch slabs strengthened by a single and double layers of ferrocement. The ferrocement layer worked together with the jack-arch slab and provided an improvement in flexural strength, stiffness, and ductility without significantly increasing the slab's weight (Resan & Dawood, 2015). The seismic performance of a jack arch slab in southern Iraq was evaluated using finite element analysis by Dawood and Resan. The results showed that flexural stresses, instead of membrane stresses, dominated the jack arch slab's behavior. According to finite element analysis, the compressive stresses developed in the slab were less than the allowable stress, but the tensile stresses were critical. Steel beam deflection and stresses were also within the permissible limits (Dawood & Resan, 2015). Flexural failure was the most common failure mode in the cellular concrete block roof structure during the test, through which the cellular concrete block unit was fractured practically in the mid-span and no crushing of the cellular concrete block due to compressive stress was noticed (Alfeehan, & Alkerwei, 2014). Ferrocement is a thin-walled reinforced concrete constructed of hydraulic cement mortar and reinforced with closely spaced layers of continuous and relatively fine wire mesh. Developing ferrocement may be traced back to Jean Louis Lambot's work in 1855 when he submitted a patent for a material he called fer-ciment (Naaman, 2000). The important advantages of employing ferrocement versus normal concrete are its lightweight, high tensile strength-to-weight ratio, and high modulus of rupture. Furthermore, raw materials are easily available (Balaguru et al., 2009). Ferrocement likely become one of the important structural alternatives to reinforced concrete in the future (Burakale et al., 2020). The flexural and compressive strength behaviors of ferrocement panels reinforced with galvanized iron mesh and polypropylene mesh were investigated. The testing results showed that polypropylene mesh panels had higher ductility qualities than galvanized iron mesh panels, and the load-bearing capability of galvanized iron and polypropylene mesh panels increased as the panel thickness and the number of mesh layers increased (Mughal et al., 2019). The development of sustainable (green) ferrocement slabs with different types of reinforcements was investigated. Cementitious materials like metakaolin and slag were used to partially replace cement. Limestone powder was employed in mortar as a partial replacement for sand. The utilization of metakaolin, slag, and limestone powder leads to the production of good mortar quality. The results also showed the modulus of rupture of ferrocement slabs increased by up to 75% when using steel wire-welded mesh of 3 mm in diameter (Jaraullah et al., 2022). The ferrocement precast slab technology achieved the best composite combination of precast and cast-in-situ systems because ferrocement precast slabs provide a lighter precast layer that enables simpler construction and transportability. By employing ferrocement as a precast layer, the system's initial structural crack load is increased, fracture probabilities during transport and handling are decreased, and the ferrocement thin section decreases the weight of the precast composite and the quantity of in-situ concrete (Yardim, 2018). A review of research on the efficiency of ferrocement confinement using stainless steel and steel meshes was conducted. The findings of the study indicated that the use of stainless steel wire mesh in ferrocement laminated can be used for rehabilitation and retrofitting concrete members prone to corrosion issues (Boban & John, 2021). Lightweight ferrocement composite plates have superior deformation, ductility, and energy absorption properties. Welded meshes have a higher modulus and hence stiffness, which results in smaller crack widths in the first region of the load-deformation curve (Shaheen et al., 2020). A fully composite action may be obtained using a shear connector to

Fig. 1 Construction of a jack arch slab by cellular concrete blocks

connect the shear loading panels of a ferrocement slab, which enhances the shear behavior (Yuvaraja et al., 2015). Experimental tests were carried out on a concrete panel sandwiched between two outer layers of reinforced concrete and joined by truss reinforcement as shear connectors. The experimental program's study found that when the thickness of the reference slab panels was increased, their strength improved. Sandwich slab panels with sawdust as aggregate in the inner wythe have stronger strength than sandwich slab panels with polystyrene (Waryosh et al., 2013). Another method to create lightweight sandwich composite components was by encasing a lightweight aerated concrete core and a high-performance ferrocement box as the skin layer. The results showed a significant increase in compressive and flexural strength. The failure mode of the sandwich components indicated ductile and composite behavior, transforming a pure brittle material (aerated concrete) into a ductile composite material because of the ferrocement encasement (Memon et al., 2006, 2007). Fahmy et al. studied using ferrocement sandwich and hollow-core panels as precast one-way slab components. Sandwich panels were constructed with two thin ferrocement layers strengthened by steel wire mesh and an autoclaved aerated lightweight concrete brick core. The results of the tests demonstrated that the recommended panels could achieve greater ultimate and service loads, fracture resistance, ductility, and energy absorption (Fahmy et al., 2012). The structural behavior of a semi-fabricated model for producing floor slabs was studied. The slab panel was composed of two layers linked together by a truss shear connection. The first layer was a formwork of precast ferrocement, while the second layer was bricks and mortar. The findings revealed that the composite slab's flexural load performance was acceptable and that it could be employed as a floor slab in construction projects (Thanoon et al., 2010). The flexural performance of a novel precast ferrocement thin panel with an inverted two-way rib as permanent formwork was studied. The results of the tests revealed that a thin panel with an adequate rib arrangement and support distance might be used as permanent formwork. The panel could resist ordinary construction workers and in-place equipment loads. The composite fullslab was able to resist normal design loads for residential construction until the ultimate load was reached, with no separation or horizontal cracks observed between the layers (Thanoon et al., 2011; Yardim et al., 2008). The use of a core material called thermocol in the building of ferrocement called "thermocol-impregnated ferrocement" was conducted. The study described the experimental investigation to understand the behavior of thermocol-impregnated ferrocement panels with various mesh layers. The results showed that thermocol-impregnated ferrocement had high flexibility, durability, workability, and heat resistance. The flexural strength and load-bearing capability improved as the number of wire meshes increased (Mazhar et al., 2021). The influence of different reinforcing types on the flexural behavior of hollow-core ferrocement slabs was investigated. Specimens of hollow-core ferrocement slabs were cast and tested until failure. The results showed that using PVC pipes as permanent hollow fillers had a significant effect on flexural strength and enhanced stiffness and ductility. The adding of steel fibers to slabs with PVC pipes increased the ultimate failure load and stiffness greatly (Naser et al., 2021). A study on the bending load on bamboo–concrete sandwich panels, steel–concrete sandwich panels, and plain concrete panels was conducted. A comparison was also made between the bamboo-concrete sandwich panel and the steel–concrete sandwich panel. The results showed that using bamboo in sandwich panels improved structural properties. Increasing face thickness from 9 to 13.5 mm increased ductility, moment capacity, and bending stiffness by 3.5, 42.1, and 127%, respectively. Furthermore, the experimental load of the bamboo-concrete sandwich panel was greater than that of the steel–concrete sandwich panel of equal weight (Fadlelmola et al., 2021). An attempt was made to reduce construction costs by inventing an Affordable Roofing System comprised of a grid including triangular main and secondary beams supporting ferrocement precast infill panels and bamboo cement precast infill panels. According to the results, the suggested Affordable Roofing System is 36.78% less expensive than a typical reinforced cement concrete roofing system (Surendra & Ravindra, 2021). Most previous studies on the jack arch slab focused on methods to strengthen it. In regards to ferrocement, the researchers focused on the structural behavior of composite and non-composite ferrocement panels, as well as the influence of various types of reinforcement and additives. From the previous works mentioned above, there have been no comprehensive studies into the behavior of ferrocement sandwich composite jack arch slabs made of two layers of ferrocement composites with styropor and cellular concrete block units as core material. So, the aim of this study is to propose a new, sustainable, and effective method for the construction of jack-arch slabs. The main idea of this method is to produce lightweight precast ferrocement elements in the form of sandwich panels to be used in the jack-arch slab between the steel I-section beam. In this study, eight specimens were manufactured and tested under three-point loads. The specimens are made of two ferrocement layers of 15 mm in thickness, separated by core material prisms (200 × 100 × 100) mm. Two different core materials are used; these are styropor or cellular concrete block (thermostone). The precast ferrocement sandwich slab has a section depth of 130 mm (15 mm for each ferrocement layer and 100 mm for the prisms). One of the specimens is made of clay brick and gypsum mortar to represent a traditional jack-arch slab and is employed as a control. The remaining seven specimens are ferrocement sandwich composite slabs.

Table 1 Clay bricks properties

Specimen type	Density (kg/m^3)	Dimension test (mm)	Average water absorption (%)		Average compressive strength (MPa)		Modulus of rupture (MPa)	Efflorescence
			10 unit	1 unit	10 unit	1 unit		
Solid Bricks	1500	233 × 113 × 72	25	25	9	8.0	2.0	Light
Limit of IQS No.25 /1993 (Class C)	–	L, W = ± 3% T = ± 4%	26	28	9	7	–	Light

Table 2 Gypsum mortar properties

Property	Test result	Limit of IQS No.28/2010
Fineness (%)	5	8% Max
Setting time (min)	13	8–25 (for jack arch using 15 max)
Compressive strength (MPa)	3	3 Min
Modulus of rupture (MPa)	0.7	–
Gypsum water ratio	0.39	–

Experimental study

Materials properties

Clay bricks are the most widely employed type of brick in jack arch slab construction. According to Iraqi specifications (IQS 25-1993), its standard dimensions are (240 × 115 × 75) mm. The bricks were tested, and the results of the tests are shown in Table 1. The gypsum mortar is a mixture of gypsum and water. The gypsum mortar was tested according to Iraqi specifications (IQS 28-2010). The results of the tests are shown in Table 2. Cellular concrete blocks (thermostone) are a type of lightweight precast cellular concrete block. Its mechanical and physical properties were tested according to Iraqi specifications (IQS 1441-2013). The results of the tests are shown in Table 3. In this work, high-density compressed styropor panels (density of styropor 20 kg/m^3) were used. The panels were (2000 × 1000 × 100) mm in size. The cellular concrete block units and the styropor panel were cut into a prism of (200 × 100 × 100) mm to the measurements necessary to make the ferrocement sandwich composite slab. For plastering purposes, cement mortar was employed on the bottom face of the jack arch slab control specimen. The cement-to-sand ratio was 1:2, with a water-to-cement ratio of 0.5. The plastering mortar has an average compressive strength of (50 × 50 × 50) mm cubes and prisms of (160 × 40 × 40) mm flexural strength of 35.7 and 7 MPa, respectively. As fine aggregate, locally available natural silica sand was employed. Its grading was tested according to (IQS No.45-1984) and the results are shown in Table 4. Drinking water was used and satisfied the standard (IQS 1703/1992).

As reinforcement for ferrocement sandwiched slabs, welded square wire mesh with a 1.0 mm wire diameter and 12.5 mm spacing was used. The mesh was tested according to the report of ACI Committee 549, which represents a design guide for the construction and repair of ferrocement. The wire mesh's yield strength was 450 MPa. The ultimate strength and modulus of elasticity of the wire mesh were 610 MPa and 93.75 GPa, respectively. For casting ferrocement sandwiched slab specimens, a different mix ratio than that used for plastering mix was used to produce a flowable, high-strength cement mortar. The water and sand to binder weight ratios were chosen to be 0.27 and 1.0, respectively. Sika viscocrete 5930L IQ was used as a high-range water reducer. The superplasticizer dosage used was 1% of the total binder weight. The average compressive and flexural strength for cubies of (50 × 50 × 50) mm and prisms (160 × 40 × 40) mm for the cement mortar that was used were 68 and 10.76 MPa, respectively.

Manufacturing of specimens

The experimental study focuses on testing one-way ferrocement sandwich composite jack arch slabs specimens. Eight samples were made, one of which was a one-way flat solid brick traditional jack arch slab with a span of 800 mm as

Table 3 Mechanical and physical properties of cellular concrete blocks

Dimension test results (mm)			Density (kg/m^3)	Compressive strength (MPa)		Modulus of rupture (MPa)
Length	Height	Thickness		One unit	Average	
+ 2	−0.5	+ 1	536.80	2.16	2.20	0.8

Table 4 Grading test result of fine aggregates

Sieve size	Cumulative retained (%)	Cumulative passing (%)	Limit of IQS No. 45/1984-Zone No. 2
10 (mm)	0	100	100
4.75 (mm)	0	100	90–100
2.36 (mm)	10	90	75–100
1.18 (mm)	13	87	55–90
600 (Micron)	45	55	35–59
300 (Micron)	72	28	8–30
150 (Micron)	94.5	5.5	0–10
Material finer than 75 micron	1.1		5% Max
Fineness modulus	2.345		(2.3–3.1) ASTM C33/86

control specimen. The remaining seven samples were precast ferrocement sandwich composite jack arch slabs specimen with varying span lengths (800, and 1000) mm, and depth of sections (130 and 160) mm, as well as varying core materials (cellular concrete blocks, and styropor) with 4 layers of wire mesh, and in a thickness of 15 mm for at both top and bottom laminates of ferrocement. Z-shaped steel wire with 3 mm in diameter were used as shear connectors in some specimens. Figure 2 shows locations of shear connectors. All samples were casted by cement mortar as one unit. Figure 3 depicts the manufacturing steps for specimens, and Fig. 4 shows graphical representation for all specimens. After 28 days and before the testing day, all specimens were cleaned, and a white painting layers were applied over the surface layer to prepare for testing and to obtain a clear view of the cracks during the test. All of the specimens' characteristics and main variables highlights in Table 5.

Testing procedure

A three-point bending load (line load) was applied to all specimens. A hydraulic jack with a capacity of 10 tons was used for testing slabs. The load was applied monotonically in equal increments and gradually increased at every load level. The slab specimen was supported on both sides by two steel rods. The deflection at mid-span was recorded using a dial gauge with a capacity of 50 mm, and the cracks have been seen using a crack microscope. A calibrated load cell has also been used to measure the load at the mid-span of a slab. Figure 5 depicts an image as well as a plan of the test setup.

Results and discussions

This section depicts and highlights the results of all tested specimens, as demonstrated in Table 6.

Ultimate load

The ultimate failure load results for all specimens are listed in Table 6. The results showed that when the span was increased from 800 to 1000 mm for SHc-4-100-0 and SHp-4-100-0, the ultimate load decreased by 23.3 and 1.19%, respectively. When the section depth of SDp-4-80-0 was increased from 130 to 160 mm, the ultimate load increased by 17.3%. Using shear connectors for SHc-4-80-0 and SHp-4-80-0 improved ultimate strength by 29.65 and 43.47%, respectively. This was because shear connectors improved interaction between the top and bottom ferrocement layers of specimens. When comparing the control specimen Js-80-0 and ferrocement sandwich slab specimens for the

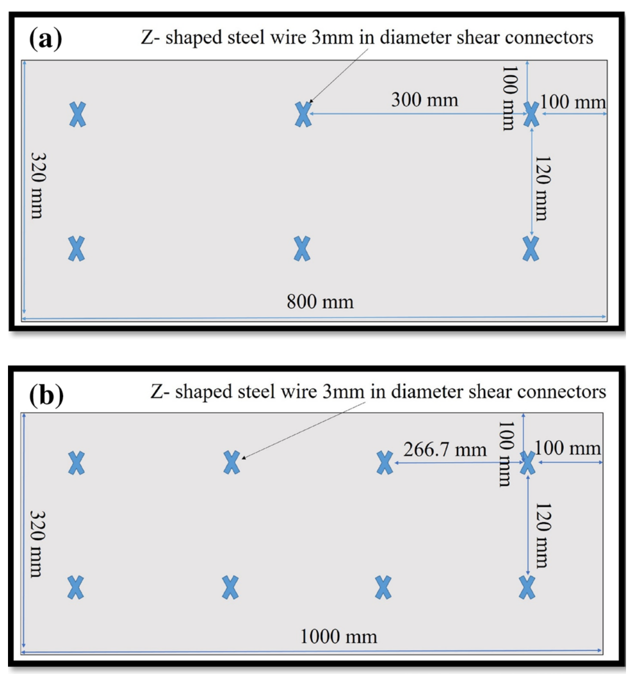

Fig. 2 Location of shear connecters. **a** Specimens with span 800 mm, **b** Specimens with span 1000 mm

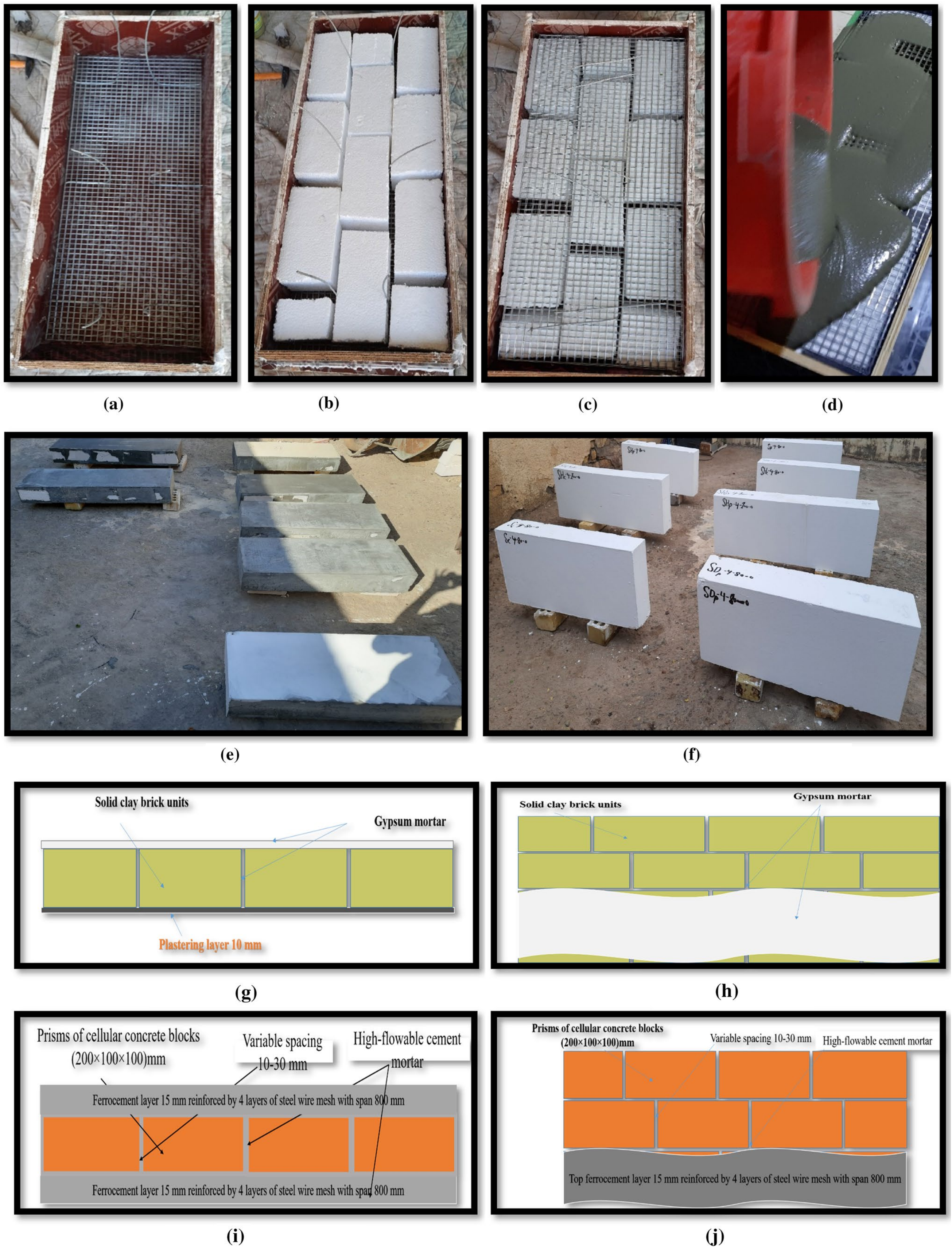

Fig. 3 Steps for made specimen. **a** Prepare mold and reinforcement cage for bottom layer. **b** Layout units of styropor or cellular concrete block. **c** Apply reinforcement cage for top layer. **d** Apply cement mortar. **e** All specimens after open molds. **f** After painting all specimens and symbols

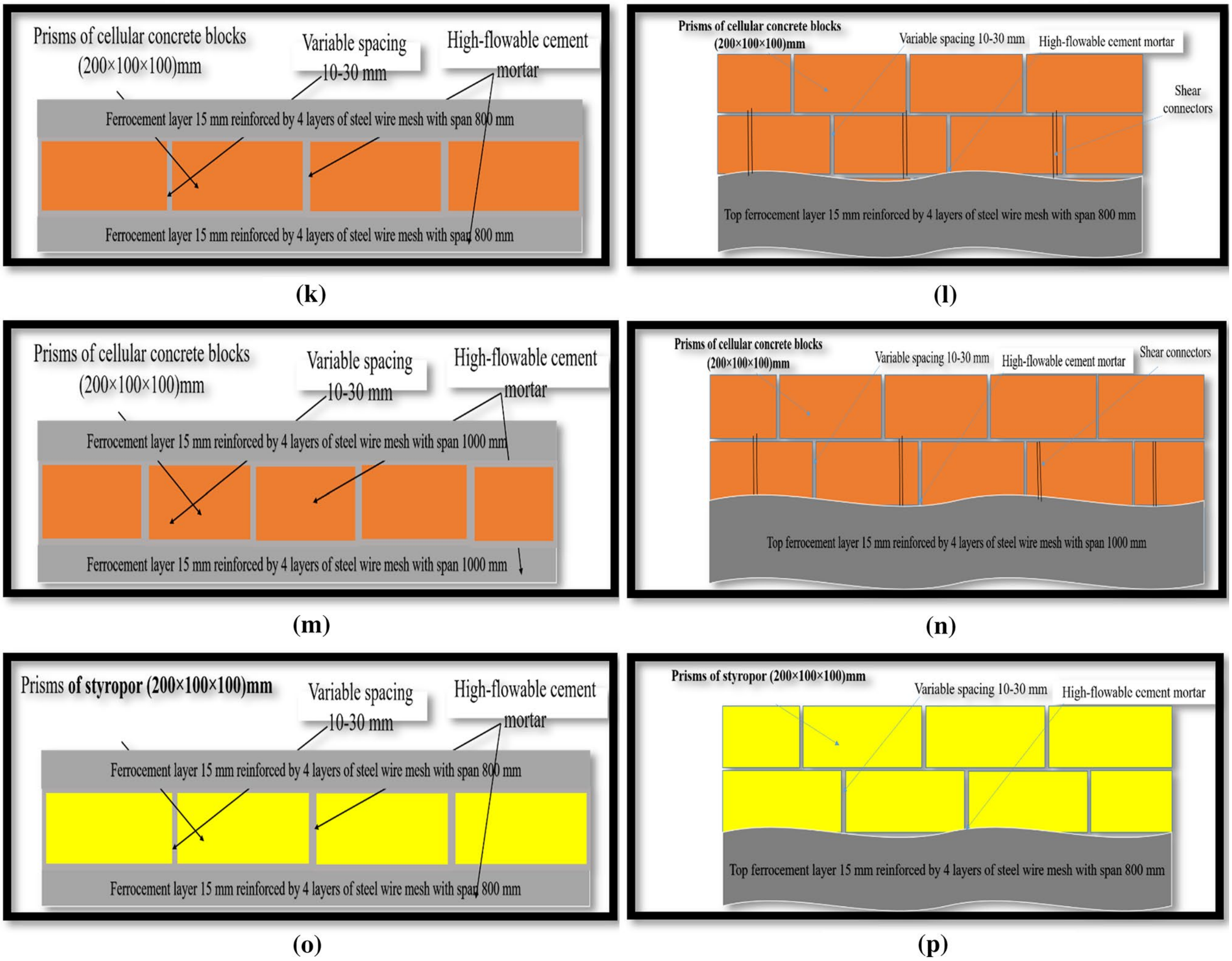

Fig. 3 (continued)

same span length, the results showed that Sc-4-80-0, SHc-4-80-0, Sp-4-80-0, SHp-4-80-0, and SDp-4-80-0 have higher ultimate strength loads than Js-80-0 by 915.7, 1216.89, 571.23, 863.01, and 1091.32%, respectively. Although SHc-4-100-0 and SHp-4-100-0 have a span length greater than control specimen Js-80-0, they have ultimate strength higher than Js-80-0 by 863.01 and 851.56%, respectively. When compared between specimens that were core materials with styropor and cellular concrete blocks for the same span and depth section, the results revealed that Sc-4-80-0, SHc-4-80-0, and SHc-4-100-0 have higher ultimate strength loads than Sp-4-80-0, SHp-4-80-0, and SHp-4-100-0 by 51.32, 36.75, and 6.14%, respectively. This was because cellular concrete block units have higher mechanical properties when compared to styropor. According to the test results, all-ferrocement sandwich composite jack arch slab specimens have a higher ultimate strength than the control jack arch slab specimen. This was due to ferrocement layers, which enhanced the slab's flexural strength.

Load–deflection curve

The load–deflection curves of all specimens are depicted in this section. Figure 6 depicts the load–deflection curve of the Js-80-0 specimen, which represents a specimen of a traditional jack arch. From this figure, it can be clearly shown that the specimen behaves approximately linearly until reaching its ultimate load. A sudden failure occurs after the formation of the first crack at this stage. Figure 7 shows load–deflection curves for Sp-4-80-0, SHp-4-80-0, SHp-4-100-0, and SDp-4-80-0 specimens, which have the same core material styropor with varying spans (800, and 1000) mm, depth sections (130, and 160) mm, and with or without shear connectors. For those specimens, three-stage load–deflection curves were seen that were different from the load–deflection curve for the control specimen. The first zone shows the linear load–deflection relationship for the uncracked stage of testing. Both the cement mortar and the reinforcement with styropor responded elastically along this

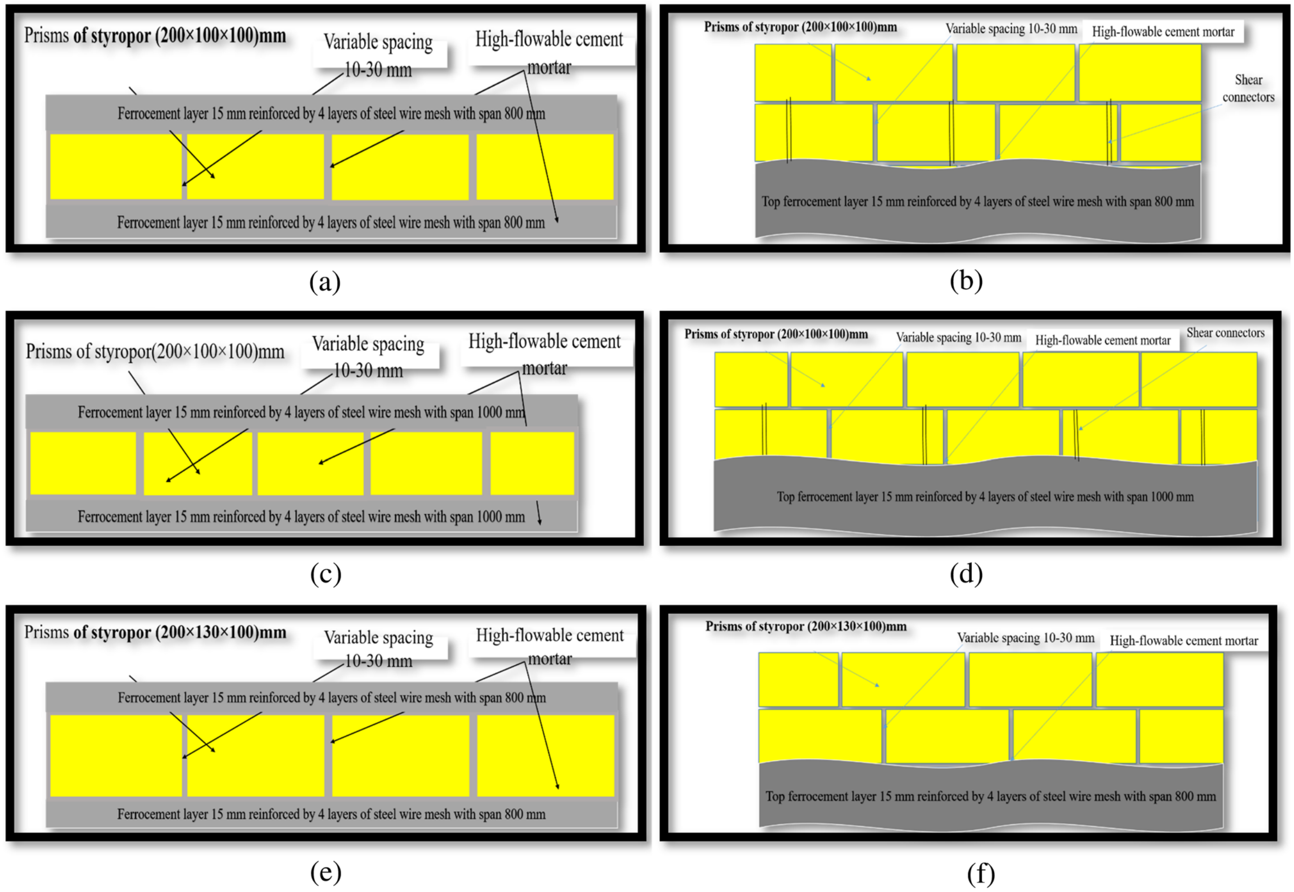

Fig. 4 Graphical representation for all specimens. **a** Front view of Js-80-0. **b** Top view of Js-80-0. **c** Front view of Sc-4-80-0. **d** Top view of Sc-4-80-0. **e** Front view of SHc-4-80-0. **f** Top view of SHc-4-80-0. **g** Front view of SHc-4-100-0. **h** Top view of SHc-4-100-0. **i** Front view of Sp-4-80-0. **j** Top view of Sp-4-80-0. **k** Front view of SHp-4-80-0. **l** Top view of SHp-4-80-0. **m** Front view of SHp-4-100-0. **n** Top view of SHp-4-100-0. **o** Front view of SDp-4-80-0. **p** Top view of SDp-4-80-0

Table 5 Details of specimens

No	Specimens symbol	No. of wire mesh layer	Volume fraction (%)	Span length (mm)	Width (mm)	Section depth (mm)	Core material type with notes
1	Js-80-0	–	–	800	320	130	Control specimen
2	Sc-4-80-0	4	3.35	800	320	130	4 layers top and bottom without shear connectors with cellular concrete blocks
3	SHc-4-80-0	4	3.35	800	320	130	4 layers top and bottom with shear connectors,and cellular concrete blocks
4	Sp-4-80-0	4	3.35	800	320	130	4 layers top and bottom without shear connectors with styropor
5	SHp-4-80-0	4	3.35	800	320	130	4 layers top and bottom with shear connectors,and styropor
6	SHc-4-100-0	4	3.35	1000	320	130	4 layers top and bottom with shear connectors, and cellular concrete blocks
7	SHp-4-100-0	4	3.35	1000	320	130	4 layers top and bottom with shear connectors,and styropor
8	SDp-4-80-0	4	3.35	800	320	160	4 layers top and bottom with shear connectors,and styropor

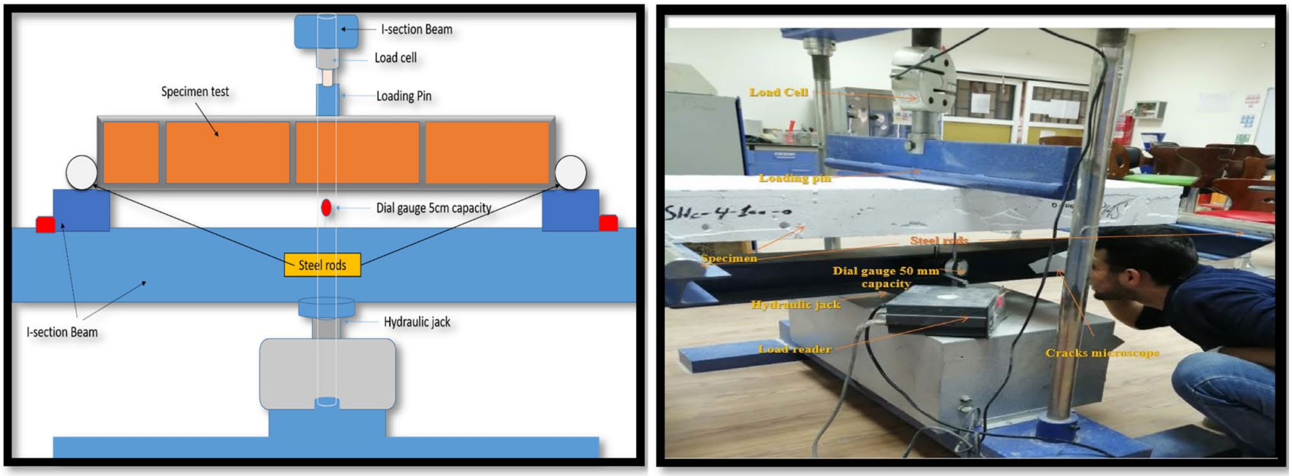

(a) (b)

Fig. 5 Flexural test setup. **a** Schematic for test setup. **b** Test setup image

Table 6 Test results of all specimens

No	Specimens symbol	Ultimate load (kN)	Ultimate deflection (mm)	Yield load (kN)	Yield deflection (mm)	First cracks load (kN)	Ductility ($\Delta u/\Delta y$)	Weight (kg)
1	Js-80-0	2.19	0.73	2.16	0.67	2.19	1.09	51
2	Sc-4-80-0	22.24	5.00	19.00	2.60	16.60	1.92	40
3	SHc-4-80-0	28.84	6.00	20.10	1.80	20.60	3.33	41
4	Sp-4-80-0	14.70	3.50	14.00	2.00	10.00	1.75	29
5	SHp-4-80-0	21.09	6.00	16.20	2.80	17.30	2.14	30
6	SHc-4-100-0	22.12	8.00	14.80	2.61	19.60	3.06	50
7	SHp-4-100-0	20.84	5.00	15.50	2.50	18.00	2.00	35
8	SDp-4-80-0	26.09	4.00	24.50	2.0	15.70	2.00	38

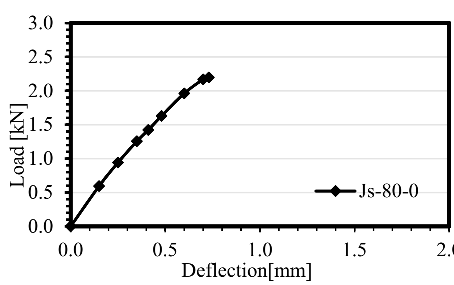

Fig. 6 Load deflection curve for Js-80-0

zone, with the cement mortar carrying most of the load. The load–deflection curve is approximately linear until the first crack load, which is indicated by the values in Table 6. The second zone starts after the first crack occurs. All specimens exhibit ductile behavior, and the number of cracks increases with increasing load, resulting in considerable deformation. The third zone is indicated by the widening of present cracks with the increase in load. Here the load is carried mainly by

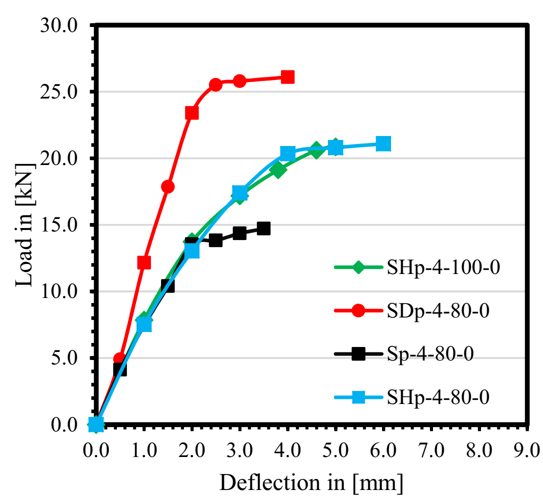

Fig. 7 Load deflection curves for Sp-4-80-0, SHp-4-80-0, SDp-4-80-0, and SHp-4-100-0

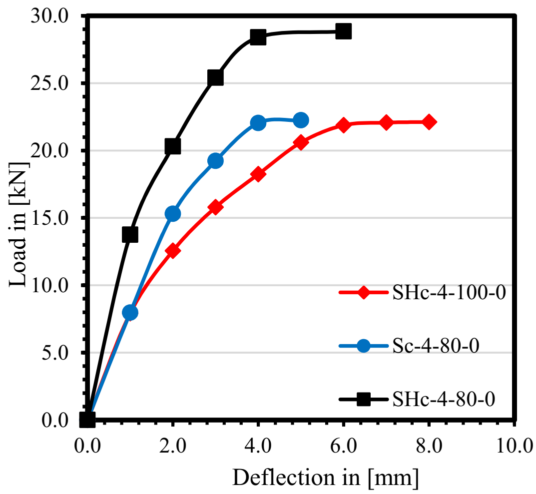

Fig. 8 Load deflection curves for Sc-4-80-0, SHc-4-80-0, and SHc-4-100-0

reinforcement. When achieving ultimate loads, specimens failed in flexural mode by fracturing the bottom layer into two pieces at a distance from the mid-span. Figure 8 depicts load–deflection curves for Sc-4-80-0, SHc-4-80-0, and SHc-4-100-0 specimens, which have the same core material as a cellular concrete block (thermostone) with varying spans (800, and 1000) mm, and with or without shear connectors. Also, for those specimens, three-stage load–deflection curves were seen that were different from the load–deflection curve for the control specimen. They were approximately similar in behavior to Sp-4-80-0, SHp-4-80-0, SHp-4-100-0, and SDp-4-80-0 specimens, in which the first zone shows the linear load–deflection relationship for the uncracked stage of testing. Both the cement mortar and the reinforcement with cellular concrete block units responded elastically along this zone, with the cement mortar carrying most of the load. The load–deflection curve is approximately linear until the first crack load, which is indicated by the values in Table 6. The second zone starts after the first crack occurs. All specimens exhibit ductile behavior, and the number of cracks increases with increasing load, resulting in considerable deformation. The third zone is indicated by the widening of present cracks with the increase in load. Here the load is carried mainly by reinforcement. When achieving ultimate loads, specimens failed in flexural mode by fracturing the bottom layer into two pieces at a distance from the mid-span.

Ductility index

The ratio of total displacement to elastic limit displacement is defined as the ductility index. The elastic limit deflection is the point at which strength behavior is assumed to change from elastic to plastic. Table 6 illustrates the ductility index

Table 7 Flexural strength and modulus results

No	Specimens symbol	Flexural strength (MPa)	Flexural modulus (MPa)
1	Js-80-0	0.48	719.71
2	Sc-4-80-0	4.93	1450.16
3	SHc-4-80-0	6.39	2503.96
4	Sp-4-80-0	3.26	1232.58
5	SHp-4-80-0	4.67	1369.87
6	SHc-4-100-0	6.13	2818.47
7	SHp-4-100-0	5.78	2790.73
8	SDp-4-80-0	3.82	1187.89

for all specimens. The control specimen of the jack arch slab had a very poor ductility index because its main elements, gypsum, clay bricks, and cement mortar, are brittle and do not have ductility properties. For sandwich ferrocement specimens, the results showed that when the span was increased from 800 to 1000 mm for SHc-4-100-0 and SHp-4-100-0, the ductility index decreased by 8.11 and 6.55%, respectively. Increased the section depth of SDp-4-80-0 from 130 to 160 mm, leading to a 14.28% increase in the ductility index. Using shear connectors for SHp-4-80-0 and SHc-4-80-0 enhanced the ductility index by 22.28 and 73.43%, respectively. When comparing the control specimen Js-80-0 and ferrocement sandwich slab specimens for the same span length, the results showed that Sc-4-80-0, SHc-4-80-0, Sp-4-80-0, SHp-4-80-0, and SDp-4-80-0 have higher ductility indexes than Js-80-0 by 76.15, 205.50, 60.55, 96.33, and 83.49, respectively. Despite SHc-4-100-0 and SHp-4-100-0 having a span length greater than control specimen Js-80-0, they have a ductility index higher than Js-80-0 by 180.73 and 83.49%, respectively. This was due to ferrocement layers that contained steel-welded wire mesh that had ductility properties higher than control specimen materials. When compared between specimens that were core materials with styropor and cellular concrete blocks for the same span and depth section, the results revealed that Sc-4-80-0, SHc-4-80-0, and SHc-4-100-0 have a higher ductility index than Sp-4-80-0, SHp-4-80-0, and SHp-4-100-0 by 9.71, 55.60, and 53.00%, respectively. According to the test results, all-ferrocement sandwich composite jack arch slab specimens have a higher ductility index than the control jack arch slab specimen. This was due to the composite behavior of the ferrocement sandwich, which converts a pure brittle material, styropor, and cellular concrete blocks into a ductile composite material. This occurred because of using ferrocement layers.

Flexural strength and modulus

Flexural strength is the ability of the material to withstand bending forces applied perpendicular to its longitudinal axis. The flexural modulus of a material is a mechanical property that measures a material's stiffness or resistance to a bending action. The flexural strength and modulus values for all specimens are calculated according to ASTM D 790-10. The results for all specimens are listed in Table 7. The results showed that the control specimen Js-80-0 of the jack arch slab had a small value of flexural strength and modulus. For sandwich ferrocement slab specimens, when the span was increased from 800 to 1000 mm for SHc-4-100-0 and SHp-4-100-0, the flexural strength decreased by 4.06% for SHc-4-100-0 and increased by 23.76% for SHp-4-100-0. The flexural modulus for the specimens SHc-4-100-0 and SHp-4-100-0 increased by 12.56 and 103.78%, respectively. Increased the section depth of SDp-4-80-0 from 130 to 160 mm, leading to a 17.17% increase in the flexural strength, while the flexural modulus decreased by 3.62%. Using shear connectors for SHp-4-80-0 and SHc-4-80-0 improved the flexural strength and modulus, by 43.25, 29.61, 11.13, and 72.66%, respectively. When comparing the control specimen Js-80-0 and ferrocement sandwich slab specimens for the same span length, the results showed that Sc-4-80-0, SHc-4-80-0, Sp-4-80-0, SHp-4-80-0, and SDp-4-80-0 have higher flexural strength and modulus than Js-80-0 by the range of (579.16–1231.25%), and (65.05–247.91%), respectively. When compared between the specimens that were core materials with styropor and cellular concrete blocks for the same span and depth section, the results revealed that Sc-4-80-0, SHc-4-80-0, and SHc-4-100-0 have flexural strength and modulus higher than Sp-4-80-0, SHp-4-80-0, and SHp-4-100-0 by 51.22, 36.83, and 6.05, 17.65, 82.78, and 1% respectively.

Failure modes

The failure mode for all specimens are shown in Fig. 9. Brittleness and the sudden collapse of brick-work arches caused by cracks at bond joints between brick units characterized failure in the control traditional jack arch slab specimen because it was the element's weakest region. This was due to the jack arch slab's composting materials being brittle and having low tensile strength. The compression face was not crushed, and the bricks did not fracture or crush during the test see Fig. 9a. Figure 9b, c, f show the mode of failure and crack pattern of sandwich ferrocement specimens Sc-4-80-0, SHc-4-80-0, and SHc-4-100-0 with core material as cellular concrete block units. Specimens failed due to reaching the ultimate stress of the reinforcing steel mesh, and the mesh bars ruptured, indicating that the strain in the steel mesh had reached its ultimate strain. Flexural cracks occurred at a distance or around the mid-span of the bottom ferrocement layers. As the applied load increased, the cracks extended vertically, resulting in the generation of additional flexural cracks. The cracks started to propagate diagonally along with the cellular concrete block units as the specimens reached their ultimate load. The diagonal pattern of cracks developed because of the poor shear resistance of the cellular concrete block units. Significant diagonal cracks occurred at the end of the specimen during failure. Horizontal separation was seen between the top and bottom ferrocement layers and the cellular concrete block units in specimens without shear connectors. No crushing of cement mortar was observed on the compression face of the cross-section. The failure mode and crack pattern of sandwich ferrocement specimens of Sp-4-80-0, SHp-4-80-0, SHp-4-100-0, and SDp-4-80-0 whose core material was styropor are shown in Fig. 9d, e, g, h. They were similar in behavior to specimens with core material of cellular concrete block units, in which specimens failed due to reaching the ultimate loads of the reinforcing steel mesh, and the mesh bars ruptured, indicating that the strain in the steel mesh had reached its ultimate strain. Flexural cracks occurred at a distance or nearer the mid-span of the bottom ferrocement layers. As the applied load increased, the cracks extended vertically, resulting in the generation of additional flexural cracks. The cracks started to propagate diagonally along with the styropor as the specimens reached their ultimate load. The diagonal pattern of cracks developed because of the poor shear resistance of the styropor. Also, significant diagonal cracks occurred at the end of the specimen during failure. Horizontal separation was seen between the top and bottom ferrocement layers and styropor in specimens without shear connectors. No crushing of cement mortar was observed on the compression face of the cross-section.

Conclusions

This study describes a novel method for producing ferrocement sandwich composite jack arch slabs made from two layers of ferrocement composites with styropor and cellular concrete block units as core materials. These slab system's specimens were tested under line loads. The study's testing results might lead to the following conclusions:

1. Ferrocement sandwich slab specimens revealed significant potential for use in a variety of construction applications and can be used for jack-arch slab applications.
2. The produced ferrocement sandwich composite jack arch slab specimens are lighter in weight than the control jack arch slab specimen of the same span and thickness. The weight decrease of the ferrocement sandwich composite jack arch slab specimens ranges from 19.6 to 43.13% depending on the core materials employed. This was

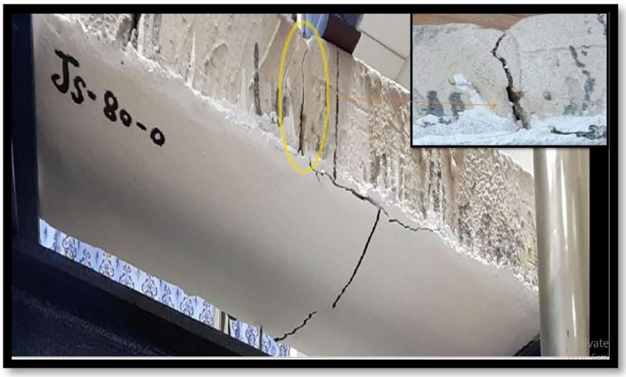

(a) Mode of failure for Js-80-0.

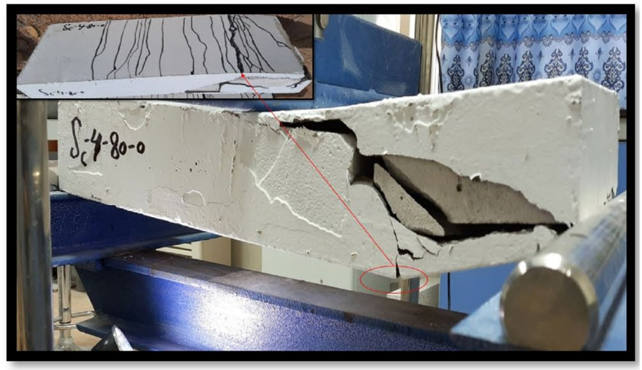

(b) Mode of failure for Sc-4-80-0.

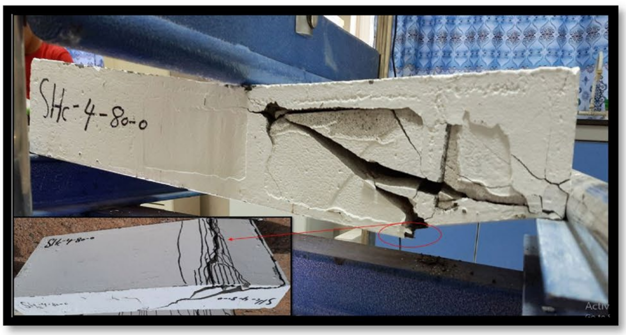

(c) Mode of failure for SHc-4-80-0.

(d) Mode of failure for Sp-4-80-0.

(e) Mode of failure for SHp-4-80-0.

(f) Mode of failure for SHc-4-100-0.

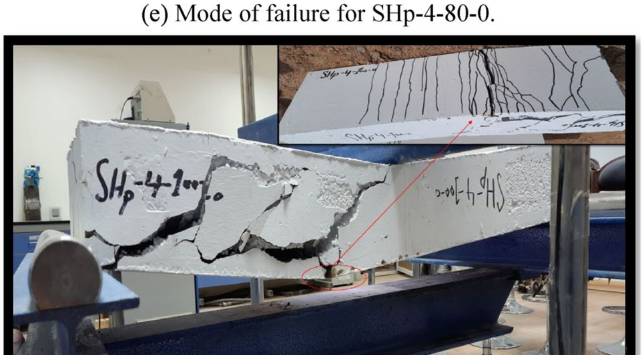

(g) Mode of failure for SHp-4-100-0.

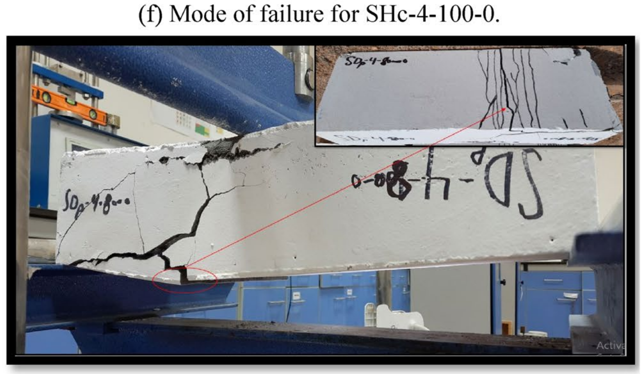

(h) Mode of failure for SDp-4-80-0.

Fig. 9 Modes of failure for all specimens. **a** Mode of failure for Js-80-0. **b** Mode of failure for Sc-4-80-0. **c** Mode of failure for SHc-4-80-0. **d** Mode of failure for Sp-4-80-0. **e** Mode of failure for SHp-4-80-0. **f** Mode of failure for SHc-4-100-0. **g** Mode of failure for SHp-4-100-0. **h** Mode of failure for SDp-4-80-0 effective in decreasing slab weight and having a positive impact on the other structural elements.

3. The manufactured ferrocement sandwich composite jack arch slab specimens exceeded structural performance of the control jack arch slab specimen, indicating that they can resist normal design loads for residential structures and can be used for jack arch slab applications.
4. The mode of failure of the ferrocement sandwich composite jack arch slab specimens indicates ductile and composite behavior, converting a pure brittle material styropor and cellular concrete blocks into a ductile composite material.
5. All ferrocement sandwich composite jack arch slab specimens have a higher ultimate strength by ranges from 471.23 to 1216.89% and ductility index by ranges from 60.55 to 205.50% than the reference jack arch slab specimen Js-80-0, respectively.
6. Ferrocement sandwich composite slab specimens have higher flexural strength and modulus than the control specimen by a range of (579.16–1231.25%), and (65.05–247.91%), respectively.
7. Using shear connectors improved ultimate strength 29.65, and 43.47%, and ductility index by 22.28, and 73.43%, respectively.
8. Increasing depth section of the ferrocement sandwich composite jack arch slab section leads to an increase in the ultimate load and ductility ratio by 77.48 and 14.28%, respectively.

Author contributions [Abdulkhaliq A. Jaafer] devised the project, the main conceptual ideas proof outline, and the measurements. [Abdulkhaliq A. Jaafer] was involved in planning and supervising the work. [Ahmed Hatif Obaid] processed the experimental data, performed the analysis, drafted the manuscript, and designed the figures. [Ahmed Hatif Obaid] manufactured the samples and characterized them. [Ahmed Hatif Obaid] performed tests and calculations. [Ahmed Hatif Obaid] listed the results and worked on the manuscript. All authors have written, discussed the results, and commented on the manuscript. All authors read and approved the final manuscript.

Funding The authors declare that no funds, grants, or other support were received during the preparation of this manuscript.

Declarations

Conflict of interest The authors declare that there are no competing interests.

References

Alfeehan, A. A., & Alkerwei, R. H. (2014). Structural behavior for low cost roof system of steel frame and thermo-stone blocks. *Engineering and Technology Journal, 32*(12 part A), 433–444.

Balaguru, P. N., Soroushian, P., Ahmad, S. H., Gale, D. M., Mobasher, B., Reddy, D. V., & Mansur, M. (2009). *Report on ferrocement*. ACI.

Boban, J. M., & John, A. S. (2021). A review on the use of ferrocement with stainless steel mesh as a rehabilitation technique. *Materials Today: Proceedings, 42*, 1100–1105.

Burakale, A. S., Attarde, P. M., & Patil, M. D. (2020). Ferrocement construction technology and its applications – a review. *International Research Journal of Engineering and Technology, 7*(7), 4178–4189.

Dawood, A. O., & Resan, S. F. (2015). Seismic analysis of traditional jack-arch slab in south of Iraq. *Al-Qadisiyah Journal for Engineering Sciences, 8*(3), 298–316.

Fadlelmola, A. B. F. A., Chen, Z., Du, Y., Ma, R., & Ma, J. (2021). December). Experimental investigation and design method on a lightweight bamboo-concrete sandwich panel under bending load. *Structures, 34*, 856–874.

Fahmy, E. H., Shaheen, Y. B., Abou Zeid, M. N., & Gaafar, H. M. (2012). Ferrocement sandwich and hollow core panels for floor construction. *Canadian Journal of Civil Engineering, 39*(12), 1297–1310.

Jaraullah, M. N. A., Dawood, E. T., & Abdullah, M. H. (2022). Static and impact mechanical properties of ferrocement slabs produced from green mortar. *Case Studies in Construction Materials, 16*, 1–12.

Maheri, M. R., Pourfallah, S., & Azarm, R. (2012). Seismic retrofitting methods for the jack arch masonry slabs. *Engineering Structure, 36*, 49–60.

Maheri, M. R., & Rahmani, H. (2003). Static and seismic design of one-way and two-way jack arch masonry slabs. *Engineering Structure, 25*(13), 1639–1654.

Mazhar, M. A., Alam, P., Kamran, M., Khan, A. H., Khan, N. A., & Ahmed, S. (2021). An experimental investigation of thermocol impregnated ferrocement panel as an alternate building material. *Materials Today: Proceedings*. https://doi.org/10.1016/j.matpr.2020.11.779

Memon, N. A., Sumadi, S. R., & Ramli, M. (2006). Strength and behaviour of lightweight ferrocement-aerated concrete sandwich blocks. *Malaysian Journal of Civil Engineering, 18*(2), 99–108.

Memon, N. A., Sumadi, S. R., & Ramli, M. (2007). Ferrocement encased lightweight aerated concrete: A novel approach to produce sandwich composite. *Materials Letters, 61*(19–20), 4035–4038.

Mughal, U. A., Saleem, M. A., & Abbas, S. (2019). Comparative study of ferrocement panels reinforced with galvanized iron and polypropylene meshes. *Construction and Building Materials, 210*, 40–47.

Naaman, A. E. (2000). *Ferrocement and laminated cementitious composites*. Techno Press.

Naser, F. H., Al Mamoori, A. H. N., & Dhahir, M. K. (2021). Effect of using different types of reinforcement on the flexural behavior of ferrocement hollow core slabs embedding PVC pipes. *Ain Shams Engineering Journal, 12*(1), 303–315.

Pourfallah, S., Maheri, M. R., & Najafgholipour, M. A. (2009). Experimental investigation of the jack arch slab retrofitted by concrete layer. *In ICCD03: 3rd International Conference on Concrete & Development* (pp. 523–533).

Resan, S. F., & Dawood, A. O. (2015). Behavior of customary jack-arch slabs in south of Iraq. *Journal of University of Babylon, 23*(2), 441–452.

Shaheen, Y. B., Eid, F. M., & Dayer, M. A. S. (2020). Developing of light weight ferrocement composite plate. *AICSGE-10*, 861–872.

Surendra, B. V., & Ravindra, R. (2021). A study of affordable roofing system using ferrocement and bamboo cement panels. *Journal of the Institution of Engineers (india), Series A, 102*(3), 633–642.

Thanoon, W. A., Yardim, Y., Jaafar, M. S., & Noorzaei, J. (2010). Structural behaviour of ferrocement–brick composite floor slab panel. *Construction and Building Materials, 24*(11), 2224–2230.

Thanoon, W. A., Yardim, Y., Jaafar, M. S., & Noorzaei, J. (2011). Structural response of interlocking composite masonry slab. *Proceedings of the Institution of Civil Engineers-Structures and Buildings, 164*(6), 409–420.

Waryosh, A. P. D. W. A., Abtan, L. D. Y. G., & Ali Dawood, M. H. (2013). Structural behavior of composite sandwich slab panels. *Journal of Engineering and Development, 17*(4), 220–232.

Yardim, Y., Jafaar, M. S., Noorzaei, J., Khan, S. R., & Kamal, N. M. (2008). Performance of precast ferrocement panel for composite masonry slab system. In *International Conference on Construction and Building Technology ICCBT* (pp. 397–407).

Yardim, Y. (2018). Review of research on the application of ferrocement in composite precast slabs. *Periodica Polytechnica Civil Engineering, 62*(4), 1030–1038.

Yuvaraja, M. R., Maheswaran, G., & Gopal, M. K. S. R. (2015). Experimental study on flexural behavior of ferrocement composite slab. *International Journal of Applied Engineering Research, 10*(57), 35–40.